arXiv:1510.04737v1 [hep-ph] 15 Oct 2015

On the rapidity dependence of the average transverse momentum in hadronic collisions

F.O. Durães,[1] A.V. Giannini,[2] V.P. Gonçalves,[3,4] and F. S. Navarra[2]

[1] *Curso de Física, Escola de Engenharia, Universidade Presbiteriana Mackenzie CEP 01302-907, São Paulo, Brazil*

[2] *Instituto de Física, Universidade de São Paulo C.P. 66318, 05315-970 São Paulo, SP, Brazil*

[3] *Instituto de Física e Matemática, Universidade Federal de Pelotas Caixa Postal 354, CEP 96010-900, Pelotas, RS, Brazil*

[4] *Department of Astronomy and Theoretical Physics, Lund University, 223-62 Lund, Sweden.*

The energy and rapidity dependence of the average transverse momentum $\langle p_T \rangle$ in pp and pA collisions at RHIC and LHC energies are estimated using the Colour Glass Condensate (CGC) formalism. We update previous predictions for the p_T - spectra using the hybrid formalism of the CGC approach and two phenomenological models for the dipole - target scattering amplitude. We demonstrate that these models are able to describe the RHIC and LHC data for the hadron production in pp, dAu and pPb collisions at $p_T \leq 20$ GeV. Moreover, we present our predictions for $\langle p_T \rangle$ and demonstrate that the ratio $\langle p_T(y) \rangle / \langle p_T(y=0) \rangle$ decreases with the rapidity and has a behaviour similar to that predicted by hydrodynamical calculations.

PACS numbers:
Keywords: Particle production, Color Glass Condensate Formalism

I. INTRODUCTION

The Large Hadron Collider (LHC) has opened up a new frontier in high energy hadron - hadron collisions, allowing to test the Quantum Chromodynamics in unexplored regimes of energy, density and rapidities, considering different configurations of the colliding hadrons (protons and nuclei) (For a recent review see e.g. [1]). In particular, the LHC experiments have unprecedented capacities to study several subjects associated to *forward physics* as, for instance, soft and hard diffraction, exclusive production of new mass states, low-x dynamics and other important topics (For a review see e.g. Ref. [2]). Forward physics is characterized by the production of particles with relatively small transverse momentum, being traditionally associated with soft particle production, which is intrinsically non perturbative and not amenable to first-principles analysis. However, in the particle production at large energies and forward rapidities, the wave function of one of the projectiles is probed at large Bjorken x and that of the other at very small x. The latter is characterized by a large number of gluons, which is expected to form a new state of matter - the Colour Glass Condensate (CGC) - where the gluon distribution saturates and non linear coherence phenomena dominate [1]. Such a system is endowed with a new dynamical momentum scale, the saturation scale Q_s, which controls the main features of particle production and whose evolution is described by an infinite hierarchy of coupled equations for the correlators of Wilson lines [3–5]. At large energies and rapidities, Q_s is expected to become much larger than the QCD confinement scale Λ_{QCD}. Furthermore, the saturation scale is expected to determine the typical transverse momentum of the produced partons in the interaction. Consequently, the probe of the average transverse momentum $\langle p_T \rangle$ in hadronic collisions can provide important information about the QCD dynamics (For related studies see, e.g. Refs. [6–8]).

Another motivation for a detailed analysis of $\langle p_T \rangle$ in pp and pA collisions is the recent suggestion made in Ref. [9] that this quantity can be used to disentangle the hydrodynamic and the CGC descriptions of the "ridge" effect (the appearance of long range correlations in the relative pseudorapidity $\Delta\eta$ and the relative azimuthal angle $\Delta\phi$ plane) observed in high multiplicity events in small colliding systems such as pp and $p(d)A$ [10–17]. While the previously ridge-type structure observed in heavy-ion collisions at RHIC and the LHC was considered as an evidence of the hydrodynamical nature of the quark-gluon-plasma, see e.g. refs. [18, 19] there is no compelling reason why small systems should also exhibit a hydrodynamical behaviour even though a hydro approach is able to describe the experimental data [20, 21]. On the other hand, the CGC approach also provides a qualitatively good description of the same data [22–32]. Therefore, the origin of the ridge in pp and pA collisions is still an open question. As the ridge effect, the azimuthal asymmetries observed in pPb collisions at the LHC energies by the ALICE [12], ATLAS [13, 33] and CMS [11, 17] collaborations are also open to different theoretical explanations. While in the hydro approaches those anisotropies emerge as a final state feature due to the hydrodynamic flow [20, 21, 34] in the CGC approach they are described as a initial state anisotropies which are present at the earliest stages of the collision [35]. In Ref. [9], the authors have studied the rapidity, y, dependence of the average transverse momentum of charged particles and found that the average transverse momentum $\langle p_T \rangle$ in CGC approach grows with rapidity, in contrast to what is expected from a collective expansion. Indeed, the hydrodynamical model predicts a decrease of the average transverse momentum when going from midrapidity, $y = 0$, to the proton side, owing to a decreasing number of produced particles. The prediction of these distinct behaviours is one the main motivations for the detailed analysis of the energy and rapidity dependencies of $\langle p_T \rangle$ and thus to verify how robust this conclusion is. Another one is to present realistic predictions for $\langle p_T \rangle$ based on the CGC results that are able to describe the current experimental data on hadron production in hadronic collisions.

This paper is organized as follows. In the next Section we present a brief review of the hybrid formalism and discuss the phenomenological models of the dipole scattering amplitudes used in our analysis. In Section III we update the main parameters of these phenomenological models by the comparison with the RHIC and LHC data on hadron production in pp, dAu and pPb collisions. Using the new version of these models, which are able to describe the experimental data for $p_T \leq 20$ GeV, we present our predictions for the rapidity and energy dependencies of the average transverse momentum in pp and pPb collisions. Finally, in Section IV we summarize our main conclusions.

II. PARTICLE PRODUCTION IN THE CGC: THE HYBRID FORMALISM

In order to estimate the energy and rapidity dependencies of the average transverse momentum $\langle p_T \rangle$ we will need to describe particle production at forward rapidities and large energies. The description of hadron production at large transverse momentum p_T is one the main examples of a hard process in perturbative QCD (pQCD). It can be accurately described within collinear factorization, by combining partonic cross-sections computed to some fixed order in perturbation theory with parton distribution and fragmentation functions whose evolution is computed by solving the Dokshitzer - Gribov - Lipatov - Altarelli - Parisi (DGLAP) equations [36] to the corresponding accuracy in pQCD. The high transverse momentum p_T of the produced hadron ensures the applicability of pQCD, which is expected to fail to low-p_T^2. Furthermore, at forward rapidities the small-x evolution becomes important, leading to a growth of the gluon density and of the gluon transverse momentum. Because of that, in this kinematical range their evolution in transverse momentum cannot be disregarded, which implies that at very forward rapidities the collinear factorization is expected to break down. An alternative is the description of hadron production using the k_T-factorization scheme, which is based on the unintegrated gluon distributions whose evolution is described by the Balitsky-Fadin-Kuraev-Lipatov (BFKL) equation [37]. However, if the transverse momentum of some of the produced particles is comparable with the saturation momentum scale, the partons from one projectile scatter off a dense gluonic system in the other projectile. In this case the parton undergoes multiple scatterings, which cannot be encoded in the traditional (collinear and k_T) factorization schemes. As pointed in Ref. [38], the forward hadron production in hadron-hadron collisions is a typical example of a dilute-dense process, which is an ideal system to study the small-x components of the target wave function. In this case the cross section is expressed as a convolution of the standard parton distributions for the dilute projectile, the dipole-hadron scattering amplitude (which includes the high-density effects) and the parton fragmentation functions. Basically, assuming this generalized dense-dilute factorization, the minimum bias invariant yield for single-inclusive hadron production in hadron-hadron processes is described in the CGC formalism by [39]

$$\begin{aligned}\frac{dN_h}{dyd^2p_T} &= \frac{K(y)}{(2\pi)^2}\int_{x_F}^{1} dx_1\,\frac{x_1}{x_F}\left[f_{q/p}(x_1,\mu^2)\,\widetilde{\mathcal{N}}_F\left(\frac{x_1}{x_F}p_T,x_2\right)\,D_{h/q}\left(\frac{x_F}{x_1},\mu^2\right)\right.\\ &\left.+\,f_{g/p}(x_1,\mu^2)\,\widetilde{\mathcal{N}}_A\left(\frac{x_1}{x_F}p_T,x_2\right)\,D_{h/g}\left(\frac{x_F}{x_1},\mu^2\right)\right]\,, \qquad (1)\end{aligned}$$

where p_T, y and x_F are the transverse momentum, rapidity and the Feynman-x of the produced hadron, respectively. The $K(y)$-factor mimics the effect of higher order corrections and, effectively, of other dynamical effects not included in the CGC formulation. The variable x_1 denotes the momentum fraction of a projectile parton, $f(x_1,\mu^2)$ the projectile parton distribution functions and $D(z,\mu^2)$ the parton fragmentation functions into hadrons. These quantities evolve according to the DGLAP evolution equations [36] and obey the momentum sum-rule. It is useful to assume $\mu^2 = p_T^2$. Moreover, $x_F = \frac{p_T}{\sqrt{s}}e^y$ and the momentum fraction of the target partons is given by $x_2 = x_1 e^{-2y}$ (For details see e.g. [39]). In Eq. (1), $\widetilde{\mathcal{N}}_F(x,k)$ and $\widetilde{\mathcal{N}}_A(x,k)$ are the fundamental and adjoint representations of the forward dipole amplitude in momentum space and are given by

$$\widetilde{\mathcal{N}}_{A,F}(x,p_T) = \int d^2r\, e^{i\vec{p_T}\cdot\vec{r}}\,[1-\mathcal{N}_{\mathcal{A},\mathcal{F}}(x,r)] \ , \tag{2}$$

where $\mathcal{N}_{\mathcal{A},\mathcal{F}}(x,r)$ encodes all the information about the hadronic scattering, and thus about the non-linear and quantum effects in the hadron wave function. Following [40], we will assume in what follows that $\mathcal{N}_F(x,r)$ can be obtained from $\mathcal{N}_A(x,r)$ after rescaling the saturation scale by $Q^2_{s,F} = (C_F/C_A)Q^2_{s,A}$ where $C_F/C_A = 4/9$. In principle, we should also include in (1) the inelastic term that has been calculated in [41]. This term accounts for part of the full next-to-leading order correction to the hybrid formalism which has been recently presented in [42, 43]. It has also been shown recently [44] that the inclusion of this term modifies the shape of the p_T spectra. However we are concerned only with the average transverse momentum $\langle p_T\rangle$ (and its rapidity dependence) and this term plays a negligible role in this observable, which is dominated by the low p_T part of the spectra. Because of this reason we will omit this term in our analysis.

The scattering amplitude $\mathcal{N}_{\mathcal{A}}(x,r)$ can be obtained by solving the BK evolution equation [3, 4] or considering phenomenological QCD inspired models to describe the interaction of the dipole with the target. The BK equation is the simplest non linear evolution equation for the dipole-hadron scattering amplitude, being actually a mean field version of the first equation of the B-JIMWLK hierarchy [3, 5]. Since the BK equation still lacks a formal solution in all kinematical space, several groups have constructed phenomenological models for the dipole scattering amplitude using the RHIC and/or HERA data to fix the free parameters [39, 40, 46, 47]. In general, it is assumed that $\mathcal{N}$ can be modelled through a simple Glauber-like formula,

$$\mathcal{N}(x,r_T) = 1-\exp\left[-\frac{1}{4}(r_T^2Q_s^2)^{\gamma}\right] \ , \tag{3}$$

where γ is the anomalous dimension of the target gluon distribution. The speed with which we move from the non linear regime to the extended geometric scaling regime and then from the latter to the linear regime is what differs one phenomenological model from another. This transition speed is dictated by the behaviour of the anomalous dimension $\gamma(x,r_T^2)$. In this paper we will consider the dipole models proposed in Refs. [39, 40] to describe the p_T spectra of particle production at RHIC. In the DHJ model [39], the anomalous dimension was proposed to be given by

$$\gamma(x,r_T)_{DHJ} = \gamma_s + (1-\gamma_s)\frac{|\log(1/r_T^2Q_s^2)|}{\lambda y + d\sqrt{y} + |\log(1/r_T^2Q_s^2)|}. \tag{4}$$

with $Q_s^2 = A^{1/3}Q_0^2(x_0/x_2)^{\lambda}$, $\gamma_s = 0.628$, $Q_0^2 = 1.0$ GeV^2, $x_0 = 3.0\cdot 10^{-4}$, $\lambda = 0.288$ and $d = 1.2$. This model was designed to describe the forward dAu data at the RHIC highest energy taking into account geometric scaling violations characterized by terms depending on the target rapidity, $y = \log(1/x_2)$, in its parametrization of the anomalous dimension, with the parameter d controlling the strength of the subleading term in y. In contrast, in the BUW model [40] the anomalous dimension is given by

$$\gamma(\omega = q_T/Q_s)_{BUW} = \gamma_s + (1-\gamma_s)\frac{(\omega^a-1)}{(\omega^a-1)+b} \ , \tag{5}$$

where $q_T = p_T/z$ is the parton momentum. The parameters of the model ($\gamma_s = 0.628$, $a = 2.82$ and $b = 168$) have been fixed by fitting the p_T-spectra of the produced hadrons measured in pp and dAu collisions at the RHIC energies [40, 48]. With these parameters the model was also able to describe the ep HERA data for the proton structure function if the light quark masses are neglected. An important feature of this model is the fact that it explicitly satisfies the property of geometric scaling [49–51] which is predicted by the solutions of the BK equation in the asymptotic regime of large energies. Since the forward RHIC data for the p_T-spectra are reproduced by both models [39, 40], it was not possible to say whether experimental data show violations of the geometric scaling or not. In principle, it is expected that by considering the transverse momentum distribution of produced hadrons measured at the LHC energies it should be possible to address this question since the new data are taken at a wider range of p_T when compared to the RHIC data.

III. RESULTS AND DISCUSSION

In what follows we will present our results for the average transverse momentum $\langle p_T\rangle$ defined by

$$\langle p_T\rangle = \frac{\int d^2p_T\, p_T\, \frac{dN_h}{dyd^2p_T}}{\int d^2p_T\, \frac{dN_h}{dyd^2p_T}} \tag{6}$$

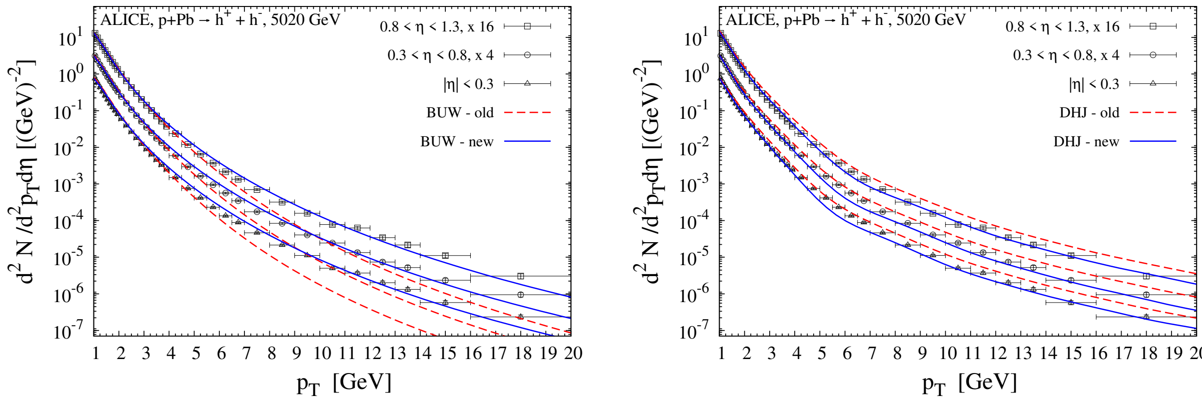

(a) (b)

FIG. 1: (Color online) Comparison between the (a) BUW and (b) DHJ predictions for the transverse momentum p_T-spectra of charged particles produced in pPb collisions and the ALICE data [52]. For the new version of the BUW model we assume $K = 3.7$ for all pseudorapidity bins and for the new DHJ model $K = 3.0$, 3.0 and 3.7 for $\langle\eta\rangle = 0$, 0.55 and 1.05, respectively.

which is rapidity and energy dependent, i.e. $\langle p_T \rangle = \langle p_T(y, \sqrt{s}) \rangle$. Moreover, it depends of the lower limit of the integrations over the transverse momentum ($p_{T,min}$). In order to obtain realistic predictions for LHC energies it is fundamental to use as input in the calculations a model which describes the experimental data on the p_T − spectra of produced particles. Consequently, as a first step we will initially compare the DHJ and BUW predictions with the recent LHC data. In Fig. 1 we present a comparison of these predictions using the original parameters, denoted "DHJ old" and "BUW old" in the figures, with the LHC data on the p_T − spectra of charged particles in pPb collisions at $\sqrt{s} = 5.02$ TeV and different rapidities [52]. We use in what follows the CTEQ6L parton distribution functions [53] and the KKP fragmentation functions [54], with the hadron mass being chosen to be the mean value of the pion, kaon and proton masses. Moreover, we compute Eq. (1) using the central values of η in the pseudorapidity ranges used in the experiment and choose $A \equiv A_{\rm min.\,bias} = 20\,(18.5)$ for pPb (dAu) collisions. We find that these models are not able to describe the ALICE data [52] at large transverse momentum with their original parameters. The natural next step is to check if a new fit of the free parameters of these models can improve the description of the experimental data. As one of the goals of our paper is to check if the average transverse momentum can be used to discriminate between the CGC and hydrodynamic descriptions of high multiplicity events observed in pPb collisions at LHC, our strategy will be the following: to determine the free parameters of the BUW and the DHJ dipole scattering amplitudes by fitting the p_T spectra of charged particles measured in pPb collisions at $\sqrt{s} = 5020$ GeV and then compare the new models with the experimental data on pp collisions at other energies and rapidities. Moreover, differently from the authors of Refs. [39, 40], who have assumed that $\gamma_s \approx 0.63$, which is the value obtained from the leading order BFKL kernel, we will consider γ_s as a free parameter. The resulting fits are shown in Figs. 1 (a) and (b) for the following parameters: $a = 2.0$, $b = 125$ and $\gamma_s = 0.74$ for the BUW model and $d = 1.0$ and $\gamma_s = 0.7$ for the DHJ model. The data are better described if we assume larger values of $\gamma_s \geq 0.7$, which is consistent with the results obtained using the renormalization group improved BFKL kernels at next-to-leading order and fixed running coupling [55]. As it can be seen, with these parameter sets our curves agree well with the experimental data. In the range $4 < p_T < 7$ GeV the DHJ curves show an "edgy" behaviour which is a reminiscence of the numerical Fourier transform. This is not a big effect and can be considered as part of the theoretical error in our calculations. It is important to emphasize that $\langle p_T \rangle$ is only marginally affected by these small oscillations (see below).

Having fixed the new parameters of the BUW and DHJ models using the experimental data on hadron production in pPb collisions, we now compare their predictions with the recent LHC data on p_T spectra of charged particles and neutral pions measured in pp collisions at different energies and distinct rapidity ranges. The only free parameter in our predictions is the K − factor, which can be energy and rapidity dependent. In what follows we will fix this parameter in order to describe the experimental data at lower p_T. In Fig. 2 we present our results. We observe that both models describe quite well the experimental data for small p_T, with the BUW predictions becoming worse at higher p_T with increasing center - of - mass energy. In contrast, the DHJ model also describes quite well data of larger p_T, which can be associated to the contribution of the geometric scaling violations taken into account in this model. As a final check, let us compare the predictions of these new versions of the phenomenological models with the RHIC data on hadron production in pp and dAu collisions in the central and forward rapidity regions. In Figs. 3 (a) and (b) we present our predictions. We find that both models describe well the experimental data at forward rapidities. On the other hand, at central rapidities, the BUW describes well the pp data for $p_T \leq 10$ GeV, but fails for $p_T \geq 3$

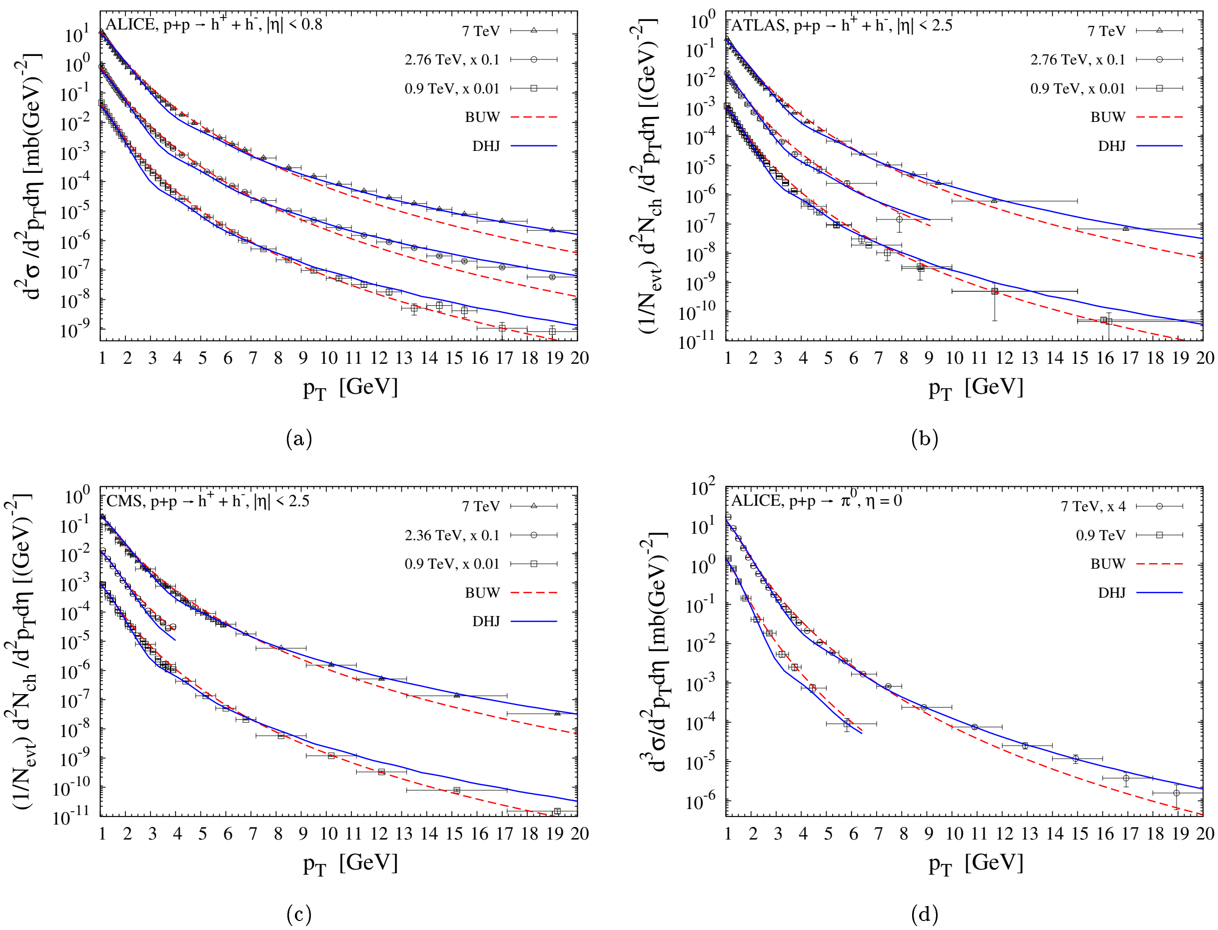

FIG. 2: (Color online) Predictions of the DHJ and BUW models for the p_T spectra of charged particles in pp collisions. (a) Comparison with the ALICE data [56]. The corresponding K factors are the following: $K = 2.47$ ($K = 2.3$), 2.07 (1.85) and 1.77 (1.6) for the BUW (DHJ) model for $\sqrt{s} = 0.9$, 2.76 and 7 TeV. (b) Comparison with the ATLAS data [57]. In this case we have assumed $K = 3.3$, 2.5 and 2.3, respectively, for both models. (c) Comparison with the CMS data [58]. In this case we assume for both models $K = 3.0$, 2.5 and 2.3 for $\sqrt{s} = 0.9$, 2.36 and 7 TeV. (d) Predictions of the DHJ and BUW models for the p_T spectra of neutral pions. Comparison with the ALICE data [59] for $\sqrt{s} = 0.9$ and 7 TeV. For both models we have $K = 1.2$ and 2.0.

GeV in the case of dAu collisions. In contrast, the results of the DHJ model are not shown for these rapidities since they are highly affected by oscilations for $p_T \gtrsim 5$ GeV. The failure of the description at central rapidities at RHIC is not surprising since the energy is not very large and the formalism used here is suited to the study of the forward region where the small-x component of the target wave function is accessed. Finally, in Fig. 3 (c) we demonstrate that the new version of the BUW model satisfies the property of the geometric scaling and also is able to describe the ep HERA data for the total $\gamma^* p$ cross section in a large range of photon virtualities.

The results presented in Figs. 1 – 3 make us confident to obtain realistic predictions for the average transverse momentum. In what follows we will study the energy and rapidity dependencies of the ratio

$$R = \frac{\langle p_T(y, \sqrt{s}) \rangle}{\langle p_T(0, \sqrt{s}) \rangle} \tag{7}$$

where the denominator represents the average transverse momentum at zero rapidity. The motivation to estimate this ratio is the reduction of the uncertainties related to the fragmentation functions as well as in the choice of the minimum transverse momentum present in the calculation of $\langle p_T \rangle$. Initially, let us analyse the dependence of our predictions on the model used to describe the forward scattering amplitudes $\mathcal{N}_{\mathcal{A},\mathcal{F}}(x,r)$. In Fig. 4 we compare the predictions of the BUW and DHJ models with those from the GBW model [63], obtained assuming $p_{T,min} = 1$ GeV. It is important to emphasize that the GBW model is not able to describe the experimental data on hadron production in hadronic collisions, since it predicts that $\mathcal{N}_{\mathcal{A},\mathcal{F}}(x,r)$ decreases exponentially at large transverse momentum. However, as this model is usually considered to obtain analytical results for several observables, we would like to verify if its

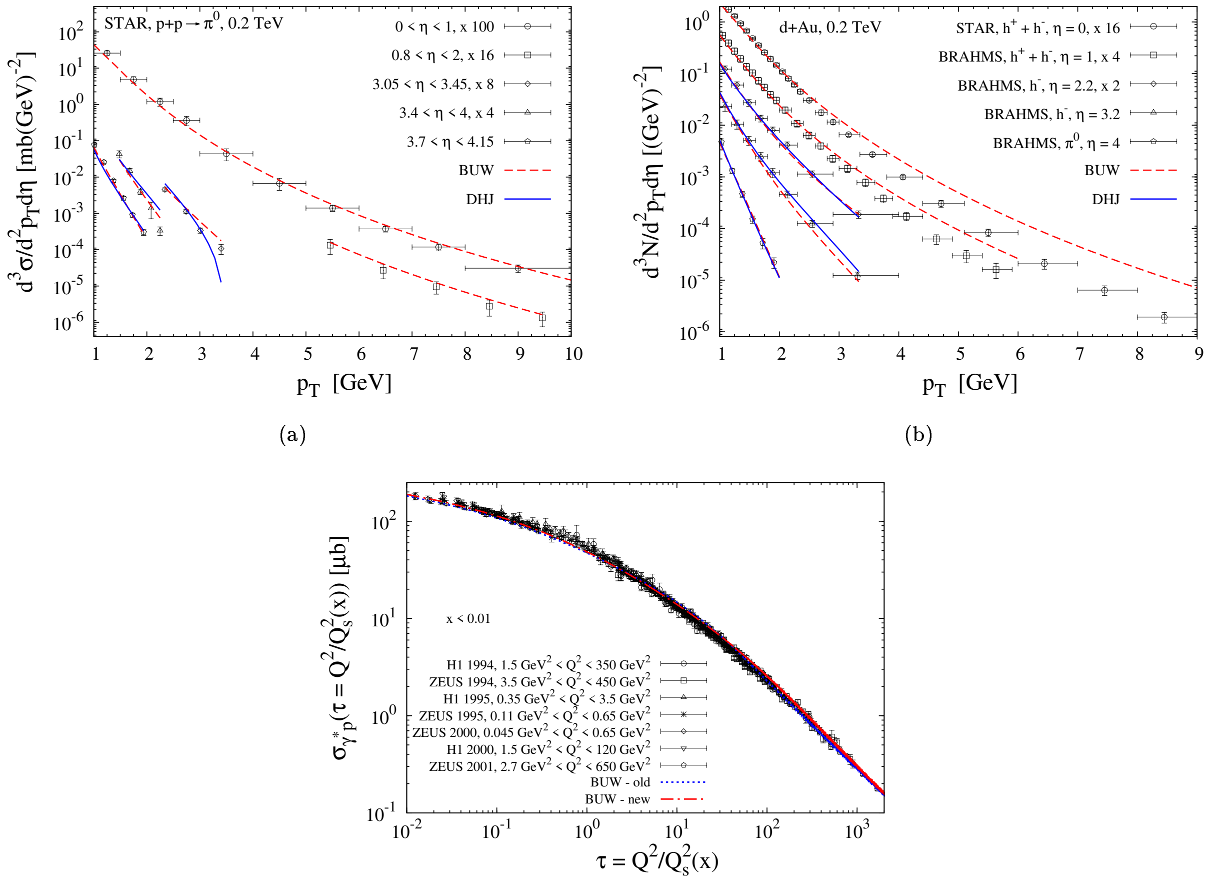

(a) (b) (c)

FIG. 3: (Color online) (a) Predictions of the DHJ and BUW models for the p_T spectra of neutral pions in pp collisions. For the BUW model $K = 1.5$ for $\langle\eta\rangle = 0.5$ and $K = 1.2$ for $\langle\eta\rangle = 1.4, 3.25, 3.7, 3.925$. For the DHJ model $K = 1.2$ for $\langle\eta\rangle = 3.25, 3.7, 3.925$. The experimental data are from [60]; (b) Predictions of the DHJ and BUW models for the p_T spectra of hadron production in dAu collisions. For the BUW model we have $K = 2.9$, 2.5, 2.0, 1.0 and 1.0 for $\eta = 0$, 1, 2.2, 3.2 and 4 respectively. For the DHJ model we have $K = 2.5$, 2.4, 1.5 for $\eta = 2.2$, 3.2 and 4 respectively. The experimental data are from [61]. (c) Comparison between the BUW predictions and the ep HERA data for the total $\gamma^* p$ cross section [62].

predictions for $\langle p_T\rangle$ are realistic. We can see that while the GBW model predicts a growth of the ratio for $y \leq 6$, the BUW and DHJ models predict the opposite, with the ratio decreasing with the rapidity. This distinct behaviour is present for pp and pPb collisions, with the behaviour of the ratio at very large rapidities being determined by kinematical constraints associated to the limited phase space. These results were obtained considering $p_{T,min} = 1$ GeV. In Fig. 5 we analyse the dependence of our results on this arbitrary cut off in the transverse momentum. For this calculation we have compared the value of the saturation scale for a given transverse momentum and rapidity with the corresponding value of p_T and assumed that the factorization scale is given by the harder scale. This basic assumption has been used in Ref. [64] in order to extend the hybrid formalism to hadron production at very small - p_T, obtaining a very good description of the LHCf data. However, it is important to emphasize that we have checked that similar results are obtained if we freeze the factorization scale at the minimum value of Q^2 allowed in the parton distributions and fragmentation functions when smaller values of p_T are probed in the calculation. The results shown in Fig. 5 indicate that the behaviour of the ratio with the rapidity is not strongly modified by the choice of $p_{T,min}$. Consequently, we will consider $p_{T,min} = 1$ GeV in what follows.

In Fig. 6 we present the behaviour the ratio $\langle p_T(y,\sqrt{s})\rangle / \langle p_T(0,\sqrt{s})\rangle$ for pp and pPb collisions considering different center of mass energies. We find that the predictions of the DHJ (red lines) and BUW (blue lines) are similar, with the DHJ being slightly larger than the BUW, and that the ratio increases with energy. Moreover, we oberve that for a fixed energy the ratio is larger for pp in comparison to pPb collisions, as demonstrated in Fig. 7 where we present our results for the ratio between the predictions for $R = \langle p_T(y,\sqrt{s})\rangle / \langle p_T(0,\sqrt{s})\rangle$ in pp collisions and those obtained for pPb collisions. Our results indicate that at very large energies the predictions for R in pp and pPb collisions become identical. These predictions are an important test of the hybrid factorization and the CGC formalism. We

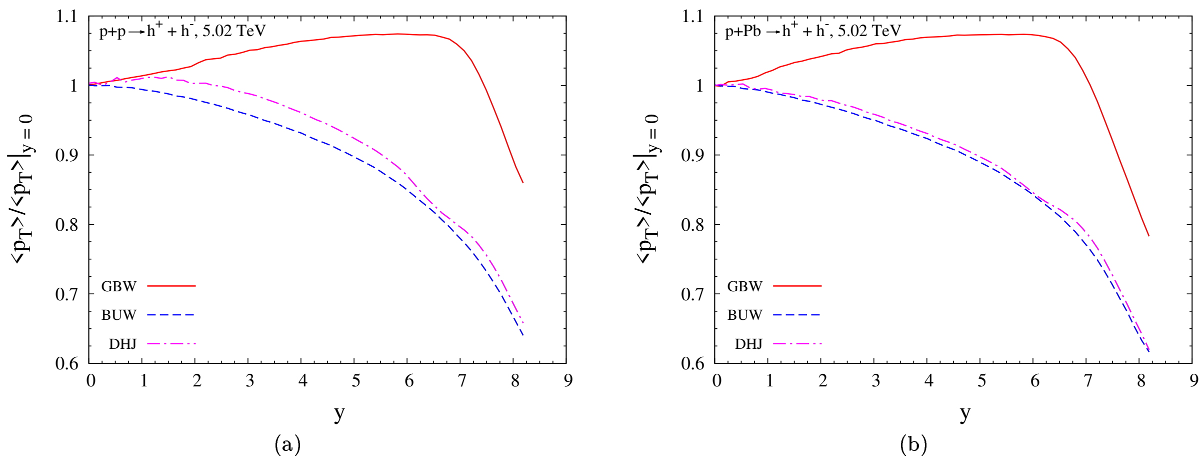

FIG. 4: (Color online) Dependence of the ratio $\langle p_T(y, \sqrt{s})\rangle / \langle p_T(0, \sqrt{s})\rangle$ in the model used for the forward scattering amplitude in (a) pp and pPb collisions.

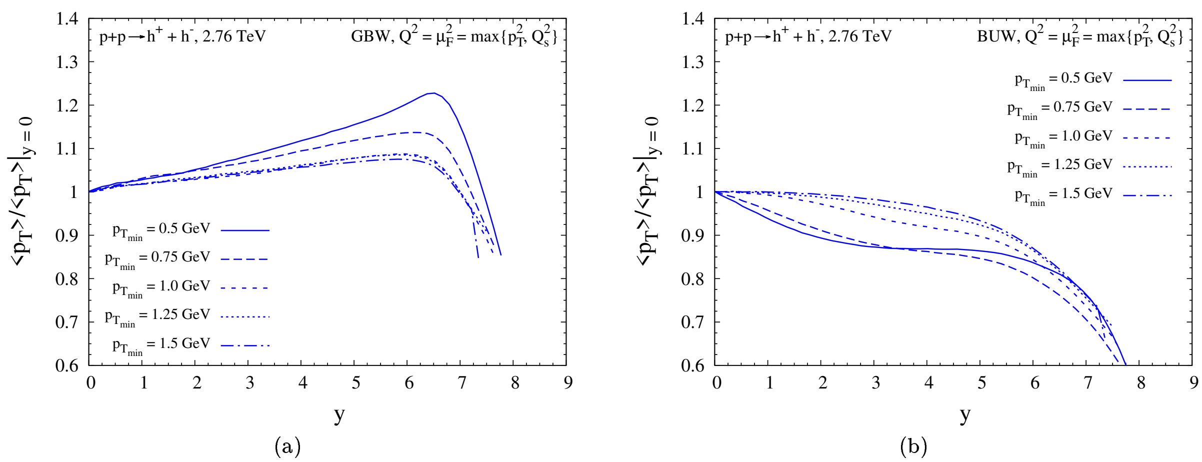

FIG. 5: (Color online) Dependence of the ratio $\langle p_T(y, \sqrt{s})\rangle / \langle p_T(0, \sqrt{s})\rangle$ in the minimum transverse momentum $p_{T,min}$ considering (a) the GBW and (b) the BUW model for the forward scattering amplitude.

believe that the analysis of the ratio R in pp and pPb collisions can be useful to probe the QCD dynamics at forward rapidities. Finally, the results from Fig. 6 indicate that the ratio decreases with the rapidity in pPb collisions for the energies probed by LHC, presenting a behaviour similar to that obtained using a hydrodynamical approach, which implies that in principle this observable cannot be used to discriminate the CGC and hydrodynamical approaches for the description of the high multiplicity events. This conclusion is opposite to that obtained in Ref. [9]. We believe that the difference of conclusions comes from the fact that in Ref. [9] the CGC results were obtained with the k_T-factorization formalism, which is reasonable for central rapidities but questionable for forward rapidities, and using an analytical approximation for the unintegrated gluon distribution that does not describe the experimental results for the p_T - spectra of hadrons produced at LHC energies. Moreover, kinematical constraints associated to the phase space restrictions at large rapidities were not included in [9]. In contrast, in our analysis we have calculated the ratio R using the hybrid formalism and two different models for the forward scattering amplitude, which we have demonstrated to be able to describe the current experimental data on charged hadron and pion p_T spectra measured in pp and pPb collisions at LHC.

IV. CONCLUSIONS

In this paper we considered the hybrid formalism to study the behaviour of the average p_T with the rapidity in pp and pPb collisions at several energies in the CGC picture of high energy collisions. In order to obtain realistic predictions we have updated previous phenomenological models for the forward scattering amplitude, one with and

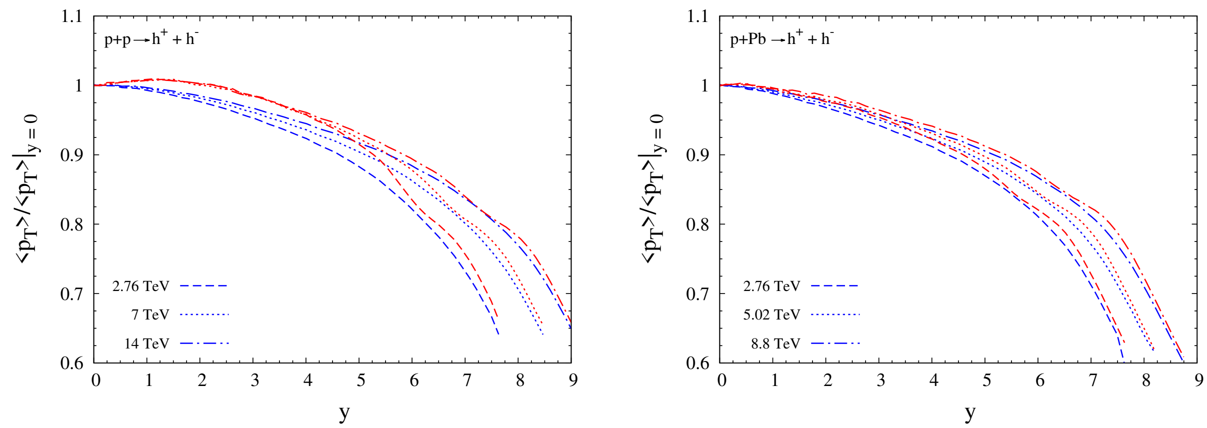

(a) (b)

FIG. 6: (Color online) Rapidity dependence of the ratio $R = \langle p_T(y, \sqrt{s})\rangle / \langle p_T(0, \sqrt{s})\rangle$ in (a) pp and (b) pPb collisions for different energies. The BUW (DHJ) predictions are represented by blue (red) lines.

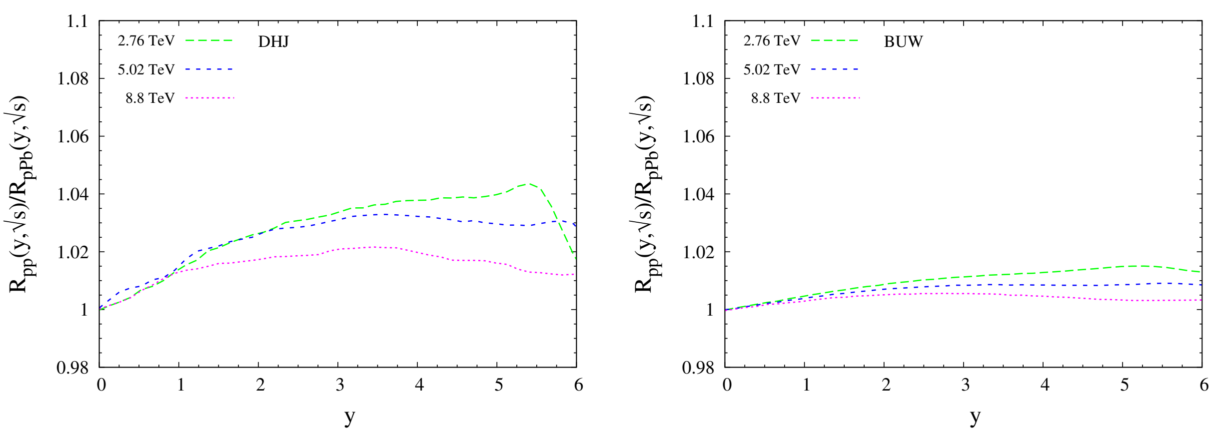

(a) (b)

FIG. 7: (Color online) Rapidity dependence of the ratio between the predictions for the $R = \langle p_T(y, \sqrt{s})\rangle / \langle p_T(0, \sqrt{s})\rangle$ in pp collisions and those for pPb collisions considering (a) the DHJ and (b) the BUW models.

other without geometric scaling violations. After constraining their parameters with the most recent data on the p_T spectra of charged particles, measured in pPb collisions at the LHC, we demonstrated that they are able to describe the recent pp data on the charged hadron and pion p_T spectra measured at LHC in the kinematical range of $p_T \leq 20$ GeV. Comparison of their predictions with the HERA and RHIC data were also presented. Using these models as input, we have calculated the average transverse momentum $\langle p_T(y, \sqrt{s})\rangle$ in pp and pPb collisions, and estimated the energy and rapidity dependencies of the $R = \frac{\langle p_T(y,\sqrt{s})\rangle}{\langle p_T(0,\sqrt{s})\rangle}$, which is an observable that can be analysed experimentally. We demonstrated that this ratio increases with the energy for a fixed rapidity and decreases with the rapidity for a fixed energy, with a behaviour similar to that predicted in hydrodynamical approaches for high multiplicity events. Finally, we demonstrated that these behaviours are almost independent of the model used for the scattering amplitude and very similar in pp and pPb collisions.

Acknowledgments

This work was partially financed by the Brazilian funding agencies CAPES, CNPq, FAPESP and FAPERGS. We thank Daniël Boer for very instructive discussions.

---

[1] F. Gelis, E. Iancu, J. Jalilian-Marian and R. Venugopalan, Ann. Rev. Nucl. Part. Sci. **60**, 463 (2010); E. Iancu and R. Venugopalan, arXiv:hep-ph/0303204; H. Weigert, Prog. Part. Nucl. Phys. **55**, 461 (2005); J. Jalilian-Marian and Y. V. Kovchegov, Prog. Part. Nucl. Phys. **56**, 104 (2006).
[2] K. Akiba et al. [The LHC Forward Physics Working Group], *LHC Forward Physics*, CERN-PH-LPCC-2015-001.
[3] I. I. Balitsky, Nucl. Phys. **B463**, 99 (1996); Phys. Rev. Lett. **81**, 2024 (1998); Phys. Rev. D **60**, 014020 (1999); Phys. Lett. B **518**, 235 (2001).
[4] Y.V. Kovchegov, Phys. Rev. D **60**, 034008 (1999); Phys. Rev. D **61** 074018 (2000).
[5] J. Jalilian-Marian, A. Kovner, L. McLerran and H. Weigert, Phys. Rev. D **55**, 5414 (1997); J. Jalilian-Marian, A. Kovner and H. Weigert, Phys. Rev. D **59**, 014014 (1999); Phys. Rev. D**59**, 014015 (1999); Phys. Rev. D **59**, 034007 (1999); E. Iancu, A. Leonidov and L. McLerran, Nucl.Phys. **A692**, 583 (2001); E. Ferreiro, E. Iancu, A. Leonidov and L. McLerran, Nucl. Phys. **A701**, 489 (2002); H. Weigert, Nucl. Phys. **A703**, 823 (2002).
[6] J. Jalilian-Marian, Nucl. Phys. A **812**, 140 (2008)
[7] L. McLerran, M. Praszalowicz and B. Schenke, Nucl. Phys. A **916**, 210 (2013)
[8] A. H. Rezaeian, Phys. Lett. B **727**, 218 (2013)
[9] P. Bozek, A. Bzdak and V. Skokov, Phys. Lett. B **728**, 662 (2014).
[10] V. Khachatryan et al. (CMS Collaboration), JHEP **09**, 091 (2010).
[11] S. Chatrchyan et al. (CMS Collaboration), Phys. Lett. B **718**, 795 (2013).
[12] B. Abelev et al. (ALICE Collaboration), Phys. Lett. B **719**, 29 (2013).
[13] G. Aad et al. (ATLAS Collaboration), Phys. Rev. Lett. **110**, 182302 (2013).
[14] B. B. Abelev et al. (ALICE Collaboration), Phys. Lett. B **726**, 164 (2013).
[15] A. Adare et al. (PHENIX Collaboration), Phys. Rev. Lett. **111**, 212301 (2013).
[16] L. Adamczyk et al. (STAR Collaboration) (2014), Phys. Lett. B **743**, 333 (2015).
[17] S. Chatrchyan et al. (CMS Collaboration), Phys. Lett. B **724**, 213 (2013).
[18] B. Alver and G. Roland, Phys. Rev. C **81**, 054905 (2010), erratum-ibid. C **82**, 039903 (2010).
[19] L. Adamczyk et al. (STAR Collaboration), Phys. Rev. C **88**, 014904 (2013).
[20] P. Bozek, Eur. Phys. J. C **71**, 1530 (2011); P. Bozek and W. Broniowski, Phys. Lett. B **718**, 1557 (2013); Phys. Rev. C **88**, 014903 (2013).
[21] P. Bozek, W. Broniowski and G. Torrieri, Phys. Rev. Lett. **111**, 172303 (2013).
[22] A. Dumitru, F. Gelis, L. McLerran, and R. Venugopalan, Nucl. Phys. A **810**, 91 (2008); S. Gavin, L. McLerran, and G. Moschelli, Phys. Rev. C **79**, 051902 (2009).
[23] A. Dumitru, K. Dusling, F. Gelis, J. Jalilian-Marian, T. Lappi and Venugopalan, Phys. Lett. B **697**, 21 (2011).
[24] A. Dumitru and J. Jalilian-Marian, Phys. Rev. D **81**, 094015.
[25] A. Kovner and M. Lublinsky, Phys. Rev. D **83**, 034017 (2011); Phys. Rev. D **84**, 094011 (2011).
[26] E. Levin and A. H. Rezaeian, Phys. Rev. D **84**, 034031 (2011).
[27] E. Iancu and D. Triantafyllopoulos, JHEP **1111** 105 (2011).
[28] K. Dusling and R. Venugopalan, Phys. Rev. D**87**, 094034 (2013); D **87**, 054014 (2013).
[29] Y. V. Kovchegov and D. E. Wertepny, Nucl.Phys. A **925**, 254 (2014).
[30] R. L. Ray, Phys. Rev. D **84**, 034020 (2011); Phys. Rev. D **90**, 5, 054013 (2014).
[31] A. Dumitru, L. McLerran and V. Skokov, Phys. Lett. B **743**, 134 (2015).
[32] A. Kovner and A. H. Rezaeian, arXiv:1508.02412 [hep-ph].
[33] G. Aad *et al.* [ATLAS Collaboration], Phys. Lett. B **725**, 60 (2013); The ATLAS collaboration, ATLAS-CONF-2014-021.
[34] P. Bozek, Phys. Rev. C **85**, 014911 (2012); A. Bzdak, B. Schenke, P. Tribedy and R. Venugopalan, Phys. Rev. C **87**, 064906 (2013); E. Shuryak and I. Zahed, Phys. Rev. C **88**, 044915 (2013); K. Werner, M. Bleicher, B. Guiot, I. Karpenko and T. Pierog, Phys. Rev. Lett. **112**, 232301 (2014); B. Schenke and R. Venugopalan, arXiv:1405.3605 [nucl-th].
[35] A. Dumitru and A. V. Giannini, Nucl. Phys. A **933**, 212 (2014); T. Lappi, Phys. Lett. B **744**, 315 (2015); B. Schenke, S. Schlichting and R. Venugopalan, Phys. Lett. B **747**, 76 (2015); A. Dumitru, A. V. Giannini and V. Skokov, arXiv:1503.03897 [hep-ph]; T. Lappi, B. Schenke, S. Schlichting and R. Venugopalan, arXiv:1509.03499 [hep-ph].
[36] Yu. Dokshitzer, Sov. Phys. JETP **46**, 641 (1977); V.N. Gribov and L.N. Lipatov, Sov. J. Nucl. Phys. **15**, 438 (1972); G. Altarelli and G. Parisi, Nucl. Phys. B **126**, 298 (1977).
[37] L. N. Lipatov, Sov. J. Nucl. Phys. **23**, 338 (1976); E. A. Kuraev, L. N. Lipatov and V. S. Fadin, Sov. Phys. JETP **45**, 199 (1977); I. I. Balitsky and L. N. Lipatov, Sov. J. Nucl. Phys. **28**, 822 (1978).
[38] E. Iancu, C. Marquet and G. Soyez, Nucl. Phys. A **780**, 52 (2006).
[39] A. Dumitru, A. Hayashigaki and J. Jalilian-Marian, Nucl. Phys. A **765**, 464 (2006); Nucl. Phys. A **770**, 57 (2006).
[40] D. Boer, A. Utermann, E. Wessels, Phys. Rev. D **77**, 054014 (2008).
[41] T. Altinoluk, A. Kovner, Phys. Rev. D **83**, 105004 (2011).

[42] G. A. Chirilli, B.-W. Xiao, F. Yuan, Phys. Rev. Lett. **108** 122301 (2012).
[43] G. A. Chirilli, B. W. Xiao and F. Yuan, Phys. Rev. D **86**, 054005 (2012).
[44] J. L. Albacete, A. Dumitru, H. Fujii and Y. Nara, Nucl. Phys. A **897**, 1 (2013).
[45] T. Lappi and H. Mntysaari, Phys. Rev. D **91**, 074016 (2015).
[46] D. Kharzeev, Y.V. Kovchegov and K. Tuchin, Phys. Lett. B **599**, 23 (2004).
[47] J. Bartels, K. Golec-Biernat, H. Kowalski, Phys. Rev. D **66**, 014001 (2002); H. Kowalski and D. Teaney, Phys. Rev. D **68**, 114005 (2003); E. Iancu, K. Itakura, S. Munier, Phys. Lett. B **590**, 199 (2004); H. Kowalski, L. Motyka and G. Watt, Phys. Rev. D **74**, 074016 (2006); V. P. Goncalves, M. S. Kugeratski, M. V. T. Machado and F. S. Navarra, Phys. Lett. B **643**, 273 (2006); C. Marquet, R. Peschanski and G. Soyez, Phys. Rev. D **76**, 034011 (2007); G. Soyez, Phys. Lett. B **655**, 32 (2007); G. Watt and H. Kowalski, Phys. Rev. D **78**, 014016 (2008).
[48] M. A. Betemps and V. P. Goncalves, JHEP **0809**, 019 (2008).
[49] A. M. Staśto, K. Golec-Biernat and J. Kwieciński, Phys. Rev. Lett. **86**, 596 (2001).
[50] C. Marquet and L. Schoeffel, Phys. Lett. B **639**, (2006) 471.
[51] V. P. Goncalves and M. V. T. Machado, Phys. Rev. Lett. **91**, 202002 (2003); V. P. Goncalves and M. V. T. Machado, JHEP **0704**, 028 (2007).
[52] B. Abelev *et al.* [ALICE Collaboration], Phys. Rev. Lett. **110**, 082302 (2013).
[53] J. Pumplin, D. R. Stump, J. Huston, H. L. Lai, P. M. Nadolsky and W. K. Tung, JHEP **0207**, 012 (2002).
[54] B.A. Kniehl, G. Kramer and B. Pötter, Nucl. Phys. B **582**, 514 (2000).
[55] G. P. Salam, JHEP **9807**, 019 (1998); M. Ciafaloni, D. Colferai and G. P. Salam, Phys. Rev. D **60**, 114036 (1999).
[56] B. B. Abelev *et al.* [ALICE Collaboration], Eur. Phys. J. C **73**, 2662 (2013).
[57] G. Aad *et al.* [ATLAS Collaboration], Phys. Lett. B **688**, 21 (2010); G. Aad *et al.* [ATLAS Collaboration], New J. Phys. **13**, 053033 (2011).
[58] V. Khachatryan *et al.* [CMS Collaboration], JHEP **1002**, 041 (2010); S. Chatrchyan *et al.* [CMS Collaboration], JHEP **1108**, 086 (2011); V. Khachatryan *et al.* [CMS Collaboration], Phys. Rev. Lett. **105**, 022002 (2010).
[59] B. I. Abelev *et al.* [ALICE Collaboration], Phys. Lett. B **717**, 162 (2012).
[60] B. I. Abelev *et al.* [STAR Collaboration], Phys. Rev. D **80**, 111108 (2009).
[61] J. Adams *et al.* [STAR Collaboration], Phys. Rev. Lett. **91**, 072304 (2003); I. Arsene *et al.* [BRAHMS Collaboration], Phys. Rev. Lett. **93**, 242303 (2004); J. Adams *et al.* [STAR Collaboration], Phys. Rev. Lett. **97**, 152302 (2006).
[62] S. Aid *et al.* [H1 Collaboration], Nucl. Phys. B **470**, 3 (1996); M. Derrick *et al.* [ZEUS Collaboration], Z. Phys. C **72**, 399 (1996); C. Adloff *et al.* [H1 Collaboration], Nucl. Phys. B **497**, 3 (1997); J. Breitweg *et al.* [ZEUS Collaboration], Phys. Lett. B **407**, 432 (1997); J. Breitweg *et al.* [ZEUS Collaboration], Phys. Lett. B **487**, 53 (2000); C. Adloff *et al.* [H1 Collaboration], Eur. Phys. J. C **21**, 33 (2001); S. Chekanov *et al.* [ZEUS Collaboration], Eur. Phys. J. C **21**, 443 (2001).
[63] K. J. Golec-Biernat, M. Wusthoff, Phys. Rev. D **59**, 014017 (1998).
[64] V. P. Goncalves and M. L. L. da Silva, Nucl. Phys. A **906**, 28 (2013)